Enantiopure and Racemic Sandwich-like Networks with Dehydration, Readsorption, and Selective Guest-Exchange Phase Transformations

ARTICLE *in* CRYSTAL GROWTH & DESIGN · NOVEMBER 2008

Impact Factor: 4.89 · DOI: 10.1021/cg800710q

5 AUTHORS, INCLUDING:

Ming-Liang Tong
Sun Yat-Sen University
286 PUBLICATIONS **12,121** CITATIONS

SEE PROFILE

Article

Enantiopure and Racemic Sandwich-like Networks with Dehydration, Readsorption, and Selective Guest-Exchange Phase Transformations

Hong-Qing Hao, Wen-Ting Liu, Wei Tan, Zhuojia Lin, and Ming-Liang Tong

Cryst. Growth Des., **2009**, 9 (1), 457-465 • DOI: 10.1021/cg800710q • Publication Date (Web): 26 November 2008

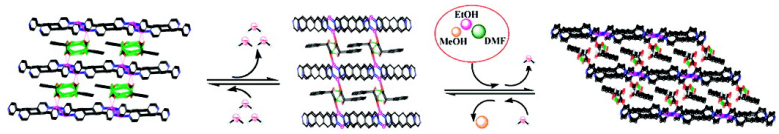

CRYSTAL GROWTH & DESIGN
2009
VOL. 9, NO. 1
457–465

Enantiopure and Racemic Sandwich-like Networks with Dehydration, Readsorption, and Selective Guest-Exchange Phase Transformations

Hong-Qing Hao, Wen-Ting Liu, Wei Tan, Zhuojia Lin,* and Ming-Liang Tong*

MOE Key Laboratory of Bioinorganic and Synthetic Chemistry, State Key Laboratory of Optoelectronic Materials and Technologies, School of Chemistry and Chemical Engineering, Sun Yat-Sen University, Guangzhou 510275, China

Received July 3, 2008; Revised Manuscript Received September 12, 2008

ABSTRACT: The room-temperature solution reactions of *R*- or *S*-H_2opa (H_2opa = 2-hydroxy-2-phenylacetic acid) with freshly prepared $[Ag(NH_3)_2](OH)$ in the presence of 1,3-di(4-pyridyl)propane (bpp) yielded two enantiomeric compounds, $[Ag_2(R\text{-Hopa})(bpp)_2](R\text{-Hopa})\cdot 3H_2O$ (**1**·$3H_2O$) and $[Ag_2(S\text{-Hopa})(bpp)_2](S\text{-Hopa})\cdot 3H_2O$ (**2**·$3H_2O$). While a similar solution reaction was carried out with racemic H_2opa instead of *R*- or *S*-H_2opa, a racemic compound $[Ag_2(R\text{-Hopa})(S\text{-Hopa})(bpp)_2]\cdot 4H_2O$ (**3**·$4H_2O$) was formed. When bulk crystals of **3**·$4H_2O$ were exposed to the air at ambient temperature, a partially dehydrated compound $[Ag_2(R\text{-Hopa})(S\text{-Hopa})(bpp)_2]\cdot H_2O$ (**4**·H_2O) was found, which would transform to $[Ag_2(R\text{-Hopa})(S\text{-Hopa})(bpp)_2]\cdot 2MeOH$ (**5**·2MeOH) by exposing the crystals of **4**·H_2O in mixed MeOH−EtOH−DMF solvent or in methanol. Compounds **1**−**5** have characteristic hydrogen-bonding-directed sandwich-like networks consisting of Ag−bpp layers and $Hopa^-$−ROH chains (R = H for **1**−**4** and Me for **5**). The different structural features come from different hydrogen bonding interactions between $Hopa^-$ and the lattice water or MeOH molecules. In **1**·$3H_2O$ and **2**·$3H_2O$, *R*-$Hopa^-$ or *S*-$Hopa^-$ form left-handed or right-handed helices with water molecules running in parallel to the Ag-bpp layers while in **3**·$4H_2O$, the centrosymmetric hydrogen bonding chains are composed of two enantiomers of $Hopa^-$. Upon dehydration, the Ag···Ag dimeric units in $[Ag_2(bpp)_2]_n^{2n+}$ in **3**·$4H_2O$ were broken and the positions of the Ag-bpp chains were adjusted to form new $Hopa^-$−H_2O chains between the silver layers. After absorbing methanol, the Ag-bpp chains restored to their original layer structures and **5**·2MeOH is pseudopolymorphic to **3**·$4H_2O$. The reversible dehydration, readsorption, and guest-exchange among **3**·$4H_2O$, **4**·H_2O, and **5**·2MeOH is an interesting example of phase transformation for racemic coordination polymers. The chirality of **1**·$3H_2O$ and **2**·$3H_2O$ was further conformed by solid-state CD spectra.

Introduction

Recent interest in crystalline homochiral materials is rapidly expanding because of their potential applications in enantioselective separation and synthesis.[1−8] Homochiral crystalline materials can be obtained through chiral synthesis using enantiomerically pure precursors, or by the resolution of racemic mixtures.[5] Recently, a chiral induction effect has been developed as an effective method to introduce chirality into materials.[7b] Under certain circumstances, enantiopure crystalline compounds can be produced spontaneously.[8] Nevertheless, the mechanism of spontaneous resolution and the formation of chiral frameworks have not been fully understood.[9−14] Intensive study of the crystallization of chiral materials from enantiopure or racemic ligands is thus necessary for the rational design of homochiral materials.

Phase transformation based on flexible networks is one of the most interesting phenomena in coordination polymers, which has attracted considerable attention in recent years because the transformation process can provide some clues to reveal the relationship between structures and properties involved. However, single crystal-to-single crystal (SC-SC) transformations are still a challenge since crystals can hardly retain their crystallinity after dramatic solid-state rearrangement of the molecules. A number of metal organic framework (MOF) SC-SC transformations in the process of guest desorption-resorption, guest-exchange, ligand exchange and thermally induced rearrangement reactions have been reported.[15−22] Sandwich-like networks have the potential to be such a kind of dynamic material as they may sustain the changes caused by external stimuli either within the layer or between the layers.

We have previously reported some silver(I)-dipyridyl-carboxylate compounds, which have typical 3D supramolecular networks constructed from Ag···Ag interaction directed $[Ag(N-N)]_n^{n+}$ coordination ladders or layers linked by carboxylate pillars.[23] As an extension of our study, chiral or racemic 2-hydroxy-2-phenylacetic acid (H_2opa) was introduced into the reaction system. Here we report the synthesis and structures of three silver(I)-dipyridyl-carboxylate compounds with chiral and racemic sandwich-like network structures as well as their phase transformation behavior via selective guest-exchange. Room temperature solution reactions of freshly prepared $[Ag(NH_3)_2](OH)$ with *R*- or *S*-2-hydroxy-2-phenylacetic acid (H_2opa) and 1,3-di(4-pyridyl)propane (bpp) in a 1:1:1 molar ratio yielded a pair of enantiomeric coordination networks, $[Ag_2(R\text{-Hopa})(bpp)_2](R\text{-Hopa})\cdot 3H_2O$ (**1**·$3H_2O$) and $[Ag_2(S\text{-Hopa})(bpp)_2](S\text{-Hopa})\cdot 3H_2O$ (**2**·$3H_2O$), respectively. Racemic compound $[Ag_2(R\text{-Hopa})(S\text{-Hopa})(bpp)_2]\cdot 4H_2O$ (**3**·$4H_2O$) was formed from a similar solution reaction when racemic H_2opa was used instead. Two derived phases, $[Ag_2(R\text{-Hopa})(S\text{-Hopa})(bpp)_2]\cdot H_2O$ (**4**·H_2O) and $[Ag_2(R\text{-Hopa})(S\text{-Hopa})(bpp)_2]\cdot 2MeOH$ (**5**·2MeOH), were obtained from **3**·$4H_2O$ via partial dehydration, reabsorption, and guest-exchange process.

Experimental Section

Materials and Physical Measurements. The reagents and solvents employed were commercially available and used as received without further purification. The C, H, and N microanalyses were carried out with Elementar Vario-EL CHNS elemental analyzer. The FT-IR spectra were recorded from KBr tablets in the range of 4000−400 cm^{-1} on a Bio-Rad FTS-7 spectrometer. Thermogravimetric (TG) analysis was

* To whom correspondence should be addressed. E-mail: tongml@mail.sysu.edu.cn (M.-L.T.), chcandy@gmail.com.

10.1021/cg800710q CCC: $40.75
Published on Web 11/26/2008

Table 1. Crystal Data and Structure Refinements for 1−5

	1 (150 K)	**2** (150 K)	**3** (298 K)	**4** (150 K)	**5** (150 K)
empirical formula	$C_{42}H_{48}O_9N_4Ag_2$	$C_{42}H_{48}O_9N_4Ag_2$	$C_{42}H_{50}O_{10}N_4Ag_2$	$C_{42}H_{44}O_7N_4Ag_2$	$C_{44}H_{50}O_8N_4Ag_2$
M	968.6	968.6	986.6	932.55	978.62
wavelength (Å)	1.54178	0.71073	0.71073	0.71073	0.71073
crystal system	monoclinic	monoclinic	monoclinic	triclinic	monoclinic
space group	$P2_1$	$P2_1$	$P2_1/c$	$P\bar{1}$	$P2_1/c$
a/Å	9.678(1)	9.6683(2)	9.865(2)	8.251(1)	9.958(1)
b/Å	8.811(1)	8.8016(2)	8.883(2)	9.642(1)	9.304(1)
c/Å	24.162(1)	24.1522(6)	25.234(5)	11.981(1)	24.884(2)
α/°	90	90	90	97.106(3)	90
β/°	93.381(2)	93.377(2)	103.380(7)	91.692(3)	112.579(5)
γ/°	90	90	90	96.596(3)	90
vol/Å^3	2056.87(7)	2051.70(8)	2151.2(8)	938.67(6)	2128.6(2)
Z	2	2	2	1	2
ρ_{calcd}/g cm^{-3}	1.564	1.568	1.523	1.650	1.527
μ/cm^{-1}	8.132	1.014	0.970	1.101	0.977
reflns collected	7866	18628	10820	9978	12956
unique reflns	4571	8607	4601	3517	4789
R_{int}	0.0212	0.0268	0.0301	0.0240	0.0482
S	1.002	0.896	1.018	1.037	0.988
R_1[a], wR_2[b] ($I > 2\sigma(I)$)	0.0242, 0.0572	0.0267, 0.0460	0.0457, 0.1095	0.0234, 0.0560	0.0326, 0.0830
R_1[a], wR_2[b] (all data)	0.0271, 0.0577	0.0396, 0.0474	0.0589, 0.1168	0.0289, 0.0572	0.0463, 0.0871
Flack parameter	−0.008(6)	−0.06(1)			

[a] $R_1 = \sum||F_o| - |F_c||/\sum|F_o|$. [b] $wR_2 = [\sum w(F_o^2 - F_c^2)^2/\sum w(F_o^2)^2]^{1/2}$.

performed at a rate of 10 °C/min under N_2 using a NETZSCH TG 209 system. The solid-state (KCl pellets) circular dichroism (CD) spectra were recorded on a JASCO J-810 spectropolarimeter.

Synthesis of [Ag$_2$(*R*-Hopa)(bpp)$_2$](*R*-Hopa)·3H$_2$O (1·3H$_2$O). Excess aqueous NH_3 solution was dropped slowly into a suspension of Ag_2O (0.046 g, 0.2 mmol) in EtOH/H_2O (15 mL, *V*/*V* = 1:1) with magnetically stirring for 15 min. *R*-H_2opa (0.061 g, 0.4 mmol) and bpp (0.079 g, 0.4 mmol) were slowly added to the silver solution. The mixture was further vigorously stirred under heating at 50 °C for 2 h. The resulting solution was filtered and allowed to stand in air at room temperature. Block colorless crystals of **1**·3H_2O were obtained after four days (yields 0.068 g, ca. 35%). Elemental analysis calcd (%) for $C_{42}H_{48}O_9N_4Ag_2$: C, 52.08; H, 5.00; N, 5.78. Found: C, 51.93; H, 4.98; N, 5.75. IR data (KBr) (400−4000 cm^{-1}): 3372(s), 3082(w), 2925(w), 2841(w), 1906(m), 1606(vs), 1575(s), 1496(m), 1451(w), 1391(m), 1258(m), 1221(w), 1187(m), 1025(s), 927(w), 840(m), 735(m), 714(m), 614(w), 511(m).

Synthesis of [Ag$_2$(*S*-Hopa)(bpp)$_2$](*S*-Hopa)·3H$_2$O (2·3H$_2$O). The procedure was similar to that used in the preparation of **1**·3H_2O except that *S*-H_2opa (0.061 g, 0.4 mmol) was used. Small block colorless crystals of **2**·3H_2O were obtained after three days. (yields 0.077 g, ca. 40%). Elemental analysis calcd (%) for $C_{42}H_{48}O_9N_4Ag_2$: C, 52.08; H, 5.00; N, 5.78. Found: C, 51.89; H, 5.03; N, 5.89. IR data (KBr) (400−4000 cm^{-1}): 3353(m), 3085(w), 2928(w), 2842(w), 1906(m), 1606(vs), 1499(w), 1356(s), 1222(m), 1054(m), 927(w), 898(w), 841(m), 735(s), 699(m), 609(m), 511(m).

Synthesis of [Ag$_2$(*R*-Hopa)(*S*-Hopa)(bpp)$_2$]·4H$_2$O (3·4H$_2$O). The procedure was similar to that used in the preparation of **1**·3H_2O except that racemic H_2opa (0.061 g, 0.4 mmol) was used. Block colorless crystals of **3**·4H_2O were obtained after three days. (yields 0.043 g, ca. 22%). Elemental analysis calcd (%) for $C_{42}H_{50}O_{10}N_4Ag_2$: C, 51.13; H, 5.11; N, 5.68. Found: C, 51.30; H, 5.01; N, 5.79. IR data (KBr) (400−4000 cm^{-1}): 3394(s), 3084(w), 2924(w), 2846(w), 1606(vs), 1499(w), 1353(s), 1223(w), 1187(w), 1088(w), 1054(m), 1025(w), 931(w), 809(m), 735(m), 698(m), 616(w), 512(m).

Synthesis of [Ag$_2$(*R*-Hopa)(*S*-Hopa)(bpp)$_2$]·H$_2$O (4·H$_2$O). Bulk crystals of **3**·4H_2O were exposed in the air at ambient temperature for about one month to produce [Ag$_2$(*R*-Hopa)(*S*-Hopa)(bpp)$_2$]·H_2O (**4**·H_2O). Elemental analysis calcd (%) for $C_{42}H_{44}O_7N_4Ag_2$: C, 54.09; H, 4.76; N, 6.01. Found: C, 54.01; H, 4.81; N, 5.93. IR (KBr, cm^{-1}): 3548(w), 3407(m), 3029(w), 2924(w), 2861(w), 1604(vs), 1496(w), 1451(w), 1421(m), 1220(w), 1190(w), 1090(w), 1060(m), 1027(w), 1007(w), 934(w), 906(w), 809(m), 737(m), 699(m), 614(w), 510(m).

Synthesis of [Ag$_2$(*R*-Hopa)(*S*-Hopa)(bpp)$_2$]·2MeOH (5·2MeOH). Crystals of [Ag$_2$(*R*-Hopa)(*S*-Hopa)(bpp)$_2$]·2MeOH (**5**·2MeOH) were obtained by exposing the crystals of **4**·H_2O in mixed MeOH−EtOH−DMF for one week. Elemental analysis calcd (%) for $C_{44}H_{50}O_8N_4Ag_2$: C, 54.00; H, 5.15; N, 5.73. Found: C, 54.15; H, 4.80; N, 5.57 IR (KBr, cm^{-1}): 3405(m), 3060(w), 3029(w), 2925(m), 2860(m), 1605(vs), 1497(m), 1455(m), 1422(s), 1359(s), 1221(m), 1190(m), 1087(m), 1057(s), 1025(m), 1007(m), 933(m), 900(m), 839(w), 809(vs), 735(m), 700(m), 614(m), 510(m).

Table 2. Selected Bond Lengths (Å) and Bond Angles (°) for 1·3H$_2$O and 2·3H$_2$O[a]

complex **1**·3H_2O		complex **2**·3H_2O	
Ag1−O1	2.584(3)	Ag1−O1	2.582(2)
Ag2−O2	2.664(6)	Ag2−O2	2.670(5)
Ag1···Ag2	2.986(1)	Ag1···Ag2	2.984(1)
Ag1−N1	2.168(4)	Ag1−N1	2.165(3)
Ag1−N3	2.172(4)	Ag1−N3	2.171(3)
Ag2−N4*a*	2.137(4)	Ag2−N4*a*	2.144(3)
Ag2−N2*b*	2.147(4)	Ag2−N2*b*	2.155(3)
N1−Ag1−N3	166.85(2)	N1−Ag1−N3	166.97(9)
N1−Ag1−O1	95.0(1)	N1−Ag1−O1	94.99(8)
N3−Ag1−O1	92.1(1)	N3−Ag1−O1	92.07(9)
N4*a*−Ag2−N2*b*	170.4(2)	N4*a*−Ag2−N2*b*	170.4(1)

[a] Symmetry codes for **1**: (a) $-x + 3$, $y - 1/2$, $-z + 1$; (b) $-x + 2$, $y - 1/2$, $-z$; symmetry codes for **2**: (a) $-x - 1$, $y + 1/2$, $-z + 1$; (b) $-x$, $y + 1/2$, $-z + 2$.

X-Ray Crystallography. Data collections were performed on Oxford Gemini S Ultra diffractometer with Cu Kα radiation ($\lambda = 1.54178$ Å) at 150 K for **1** and on Bruker Apex CCD diffractometer with Mo Kα radiation ($\lambda = 0.71073$ Å) at 150(2) or 293(2) K for **2**−**5**. The intensities were integrated with SAINT$^+$, which were also applied corrections for Lorentz and polarization effects. Absorption corrections were applied by using the multiscan program SADABS.[24] The structures were solved by direct methods. All non-hydrogen atoms were refined anisotropically by least-squares method on F^2 using the SHELXTL program.[25] The organic hydrogen atoms were generated geometrically (C_{aryl}−H 0.93 Å; C_{alkyl}−H 0.97 Å); the aqua hydrogen atoms were located from difference maps and refined with isotropic temperature factors. Crystal data as well as details of data collection and refinements for compounds **1**−**5** are summarized in Table 1. Selected bond distances are listed in Tables 2 and 3. Hydrogen bond distances and angles are listed in Tables 4−8.

Results and Discussion

Synthesis. It is well-known that different sources of the reactant components, for example, the utilization of many metal salts or using various organic precursors instead of the target ligands, have great influence on the resulted products. The reactions of silver(I) salts and organic ligands with carboxylic groups in aqueous solution often lead to microcrystalline or

Table 3. Selected Bond Lengths (Å) and Bond Angles (°) for 3·4H$_2$O, 4·H$_2$O, and 5·2MeOH[a]

complex **3**·4H$_2$O			
Ag1−O1	2.644(4)	Ag1−N2*b*	2.179(3)
Ag1−O2	2.673(3)	Ag1−N1	2.166(3)
Ag1···Ag1*a*	3.223(1)		
N1−Ag1−N2*b*	159.6(1)	N1−Ag1−O1	103.6(1)
N2*b*−Ag1−O1	95.6(1)	N1−Ag1−O2	94.4(1)
N2*b*−Ag1−O2	93.2(1)	O1−Ag1−O2	48.9(1)
complex **4**·H$_2$O			
Ag1−O1	2.478(2)	Ag1−N1	2.248(2)
Ag1−O2	2.637(2)	Ag1−N2*a*	2.239(2)
Ag1···Ag1*b*	4.902(6)		
N2*a*−Ag1-N1	132.61(6)	N2*a*−Ag1-O1	96.95(6)
N1−Ag1−O1	119.61(6)	N2*a*−Ag1-O2	139.43(6)
N1−Ag1−O2	87.92(6)	O1−Ag1−O2	51.46(5)
complex **5**·2MeOH			
Ag1−O1	2.644(2)	Ag1−N2*b*	2.188(1)
Ag1−O2*c*	2.745(1)	Ag1−N1	2.200(1)
Ag1···Ag1*a*	2.921(1)		
N2*b*−Ag1−N1	166.20(7)	N2*b*−Ag1−O1	93.82(7)
N1−Ag1−O1	93.50(7)		

[a] Symmetry codes for **3**: (a) $-x+1$, $y-3/2$, $-z+1/2$; (b) x, $-y-3/2$, $z-1/2$; symmetry codes for **4**: (a) $-x-1$, y, $z-1$; (b) $-x+1$, $-y+1$, $-z-1$; symmetry codes for **5**: (a) $-x+1$, $y+1/2$, $-z+1/2$; (b) $x-1$, $-y+3/2$, $z-1/2$, (c) $-x+1$, $-y$, $-z$.

Table 4. Hydrogen Bonds for [Ag$_2$(*R*-Hopa)(bpp)$_2$]·(*R*-Hopa)·3H$_2$O (1·3H$_2$O)[a]

D−H···A	*d*(D−H)	*d*(H···A)	*d*(D···A)	∠(DHA)
O(3)−H(3O)···O(3W)	0.84(2)	2.14(2)	2.958(6)	162(5)
O(6)−H(6O)···O(5)	0.84(2)	2.04(7)	2.579(5)	121(7)
O(1W)−H(1WA)···O(4)	0.85(2)	2.28(3)	3.052(6)	152(5)
O(1W)−H(1WA)···O(5)	0.85(2)	2.33(3)	3.092(6)	149(5)
O(1W)−H(1WB)···O(3*a*)	0.86(2)	2.05(2)	2.902(6)	173(7)
O(2W)−H(2WA)···O(2*b*)	0.86(2)	1.94(3)	2.772(6)	163(6)
O(2W)−H(2WB)···O(4*c*)	0.86(2)	1.89(3)	2.724(7)	164(8)
O(3W)−H(3WA)···O(2W)	0.86(2)	1.91(2)	2.771(7)	176(6)
O(3W)−H(3WB)···O(1)	0.88(2)	1.95(3)	2.776(6)	156(6)

[a] Symmetry codes: (a) $x+1$, y, z; (b) x, $y+1$, z; (c) $x-1$, $y+1$, z.

Table 5. Hydrogen Bonds for [Ag$_2$(*S*-Hopa)(bpp)$_2$]·(*S*-Hopa)·3H$_2$O (2·3H$_2$O)[a]

D−H···A	*d*(D−H)	*d*(H···A)	*d*(D···A)	∠(DHA)
O(3)−H(3O)···O(3W)	0.85(2)	2.11(2)	2.952(4)	169(4)
O(6)−H(6O)···O(5)	0.84(2)	2.04(3)	2.568(4)	120(2)
O(1W)−H(1WB)···O(4)	0.83(2)	2.29(3)	3.036(4)	150(4)
O(1W)−H(1WB)···O(5)	0.83(2)	2.34(3)	3.099(5)	153(4)
O(1W)−H(1WA)···O(3*a*)	0.84(2)	2.12(2)	2.901(3)	153(3)
O(2W)−H(2WA)···O(2*b*)	0.83(2)	1.98(2)	2.765(3)	159(4)
O(2W)−H(2WB)···O(4*c*)	0.83(2)	1.92(2)	2.741(4)	169(4)
O(3W)−H(3WB)···O(2W)	0.85(2)	1.93(2)	2.774(4)	174(4)
O(3W)−H(3WA)···O(1)	0.88(2)	1.91(2)	2.778(4)	169(5)

[a] Symmetry codes: (a) $x-1$, y, z; (b) x, $y-1$, z; (c) $x+1$, $y-1$, z.

Table 6. Hydrogen Bonds for [Ag$_2$(*R*-Hopa)(*S*-Hopa)(bpp)$_2$]·4H$_2$O (3·4H$_2$O)[a]

D−H···A	*d*(D−H)	*d*(H···A)	*d*(D···A)	∠(DHA)
O(3)−H(3)···O(1*a*)	0.82	2.13	2.894(6)	154.4
O(1W)−H(1WA)···O(1)	0.85(2)	1.90(2)	2.74(1)	175(7)
O(1W)−H(1WB)···O(2W*b*)	0.84(2)	1.99(2)	2.79(1)	159(5)
O(2W)−H(2WA)···O(2)	0.85	1.99	2.753(7)	148.8
O(2W)−H(2WB)···O(1W*a*)	0.85	2.41	3.21(1)	157.1

[a] Symmetry codes: (a) $-x$, $-y-2$, $-z$; (b) x, $y-1$, z.

amorphous insoluble 'silver complexes', which is presumably due to the formation of polymeric structures via rapid interactions between carboxylic groups and silver ions. There is still a general challenge in growing single crystals of desired materials with suitable size for X-ray structural analysis. Controlled release of silver ions may help to slow down the formation of silver-organic coordination frameworks and grow better single crystals. For example, Mak and co-workers used various zwitterionic betaine ligands to yield a number of polymeric silver(I) carboxylates compounds.[26] Smith and co-workers obtained a series of Ag multicarboxylate compounds from ammonia solutions[27] and Michaelides and co-workers reported a novel succinatodisilver(I) complex prepared via gel permeation method.[28] We have used freshly synthesized [Ag(NH$_3$)$_2$](OH) to react with multicarboxylic acid ligands, such as 1,2,3,4,5,6-cyclohexanehexacarboxylic acid and 1,3,5-cyclohexanetricarboxylic acid, and successfully obtained some interesting polymeric coordination compounds.[29] In this study, we fixed the molar ratio of [Ag(NH$_3$)$_2$](OH)/H$_2$opa/bpp to 1:1:1 and investigated how the chirality of H$_2$opa ligands impacts on supramolecular architectures of the Ag−Hopa$^-$−bpp system. As expected, **1**·3H$_2$O, **2**·3H$_2$O, and **3**·4H$_2$O were obtained from the room-temperature solution reactions of freshly prepared [Ag(NH$_3$)$_2$](OH), *R*-H$_2$opa (or *S*-H$_2$opa or *rac*-H$_2$opa) and bpp in a 1:1:1 molar ratio. As these reactions were carried out at ambient temperature under mild reaction conditions, the racemization of the chiral H$_2$opa ligands, which might happen at high temperatures as reported,[30,31] could be efficiently avoided.

Phase Transformation among 3·4H$_2$O, 4·H$_2$O, and 5·2MeOH via Partial Dehydration, Readsorption, and Guest-Exchange. The crystals of **1**·3H$_2$O and **2**·3H$_2$O lost crystallinity after exposed in air for several days. Comparatively, the bulky sample of **3**·4H$_2$O slowly transformed to the partially dehydrated compound **4**·H$_2$O when exposed in air at ambient temperature for about one month. **4**·H$_2$O has a much smaller unit cell in triclinic space $P\bar{1}$ and is apparently a more condensed phase than **3**·4H$_2$O. The phase transformation between **3**·4H$_2$O and **4**·H$_2$O is reversible and when **4**·H$_2$O was soaked in aqueous solution for two weeks, crystalline **3**·4H$_2$O was yielded.

Crystals of **5**·2MeOH were obtained by exposing the crystals of **4**·H$_2$O in MeOH for one week or in mixed MeOH−EtOH−DMF solvent. Single crystal X-ray crystallography shows that **5**·2MeOH has almost the same unit cell and the same space group as **3**·4H$_2$O, suggesting that **3**·4H$_2$O and **5**·2MeOH have similar coordination networks and supramolecular packing. After absorbing two methanol molecules per formula, the condensed framework of **4**·H$_2$O changed back to the phase with larger void space. It is interesting that **4**·H$_2$O can also be formed again when bulky **5**·2MeOH was exposed to wet air at ambient temperature for one week. The processes above can be monitored by single crystal and powder X-ray diffraction. The schematic representation of the reactions, dehydration, readsorption, and guest-exchange were summarized in Scheme 1.

Table 7. Hydrogen Bonds for [Ag$_2$(*R*-Hopa)(*S*-Hopa)(bpp)$_2$]·H$_2$O (4·H$_2$O)[a]

D−H···A	*d*(D−H)	*d*(H···A)	*d*(D···A)	∠(DHA)
O(3)−H(3O)···O(2)	0.82(2)	2.16(2)	2.644(2)	118(2)
O(3)−H(3O)···O(2*a*)	0.82(2)	2.28(2)	2.976(2)	142(2)
O(1W)−H(1WA)···O(1)	0.85	1.97	2.744(4)	151.3
O(1W)−H(1WB)···O(1*b*)	0.85	2.14	2.919(4)	151.9

[a] Symmetry codes: (a) $-x+1$, $-y$, $-z+1$; (b) $-x+1$, $-y$, $-z$.

Table 8. Hydrogen Bonds for [Ag$_2$(*R*-Hopa)(*S*-Hopa)(bpp)$_2$]·2MeOH (5·2MeOH)

D−H···A	*d*(D−H)	*d*(H···A)	*d*(D···A)	∠(DHA)
O(3)−H(3O)···O(1)	0.85(2)	2.00(3)	2.554(3)	122(3)
O(4)−H(4O)···O(2)	0.86(2)	1.93(3)	2.739(5)	155(6)

Scheme 1. Schematic Representation of the Phase Transformation of 3·4H$_2$O via Dehydration, Readsorption, and Guest-Exchange

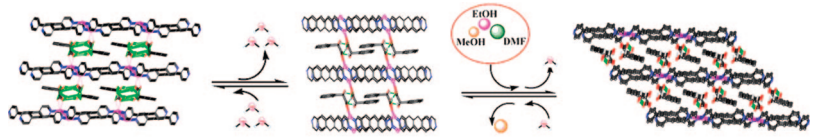

3·4H$_2$O 4·H$_2$O 5·2MeOH

Crystal Structures. Structures of [Ag$_2$(*R*-Hopa)(bpp)$_2$](*R*-Hopa)·3H$_2$O (1·3H$_2$O) and [Ag$_2$(*S*-Hopa)(bpp)$_2$](*S*-Hopa)·3H$_2$O (2·3H$_2$O). 1·3H$_2$O and 2·3H$_2$O are enantiomers. Each asymmetric unit contains one dimeric $[Ag_2(bpp)_2]^{2+}$ cation, one coordinated and one free Hopa$^-$ anion (*R*-Hopa in 1·3H$_2$O and *S*-Hopa in 2·3H$_2$O), and three guest water molecules. All the Ag(I) ions have the T-shaped coordination geometry surrounded by two nitrogen atoms from two bpp ligands and one weakly coordinated carboxylate group from *R*-Hopa$^-$ or *S*-Hopa$^-$ (Figure 1a,b).

In 1·3H$_2$O, two crystallographically distinctive Ag atoms, Ag1 and Ag2, are linked by two bpp ligands [Ag1−N = 2.168(4) and 2.172(4) Å, Ag2−N = 2.137(4) and 2.147(4) Å] and form an infinite $[Ag(bpp)]_n$ chain along the *c* axis. The adjacent Ag-bpp chains are aligned in parallel and bridged into a 2D coordination layer by carboxylate groups from Hopa$^-$ [Ag1−O1 = 2.584(3) Å, Ag2−O2 = 2.664(6) Å]. The Ag···Ag separation is 2.986(1) Å (Figure 1c), much shorter than van der Waals radii of two silver ions (3.44 Å).[32,33] The Hopa$^-$ ligands stand alternatively on both sides of the coordination layer along the silver-pyridine chains. Notably, the coordinated Hopa$^-$ on the $[Ag_2(bpp)_2]^{2+}$ dimer on adjacent silver-pyridine chains extend in the same direction and form 1D hydrogen-bonded helical with the free R-Hopa$^-$ and lattice water molecules along the *a*-axis between the layers. Each helical step contains one coordinated and one lattice *R*-Hopa$^-$ anion linked by two water molecules with the pitch of 8.811(1) Å [O2W···O2 = 2.772(6) Å, O2W−H2WA···O2 = 163(6)°; O3W···O1 = 2.776(6) Å, O3W−H3WB···O1 = 156(6)°; O3W···O2W = 2.771(7) Å, O3W−H3WA···O2W = 176(6)°] (Figure 1d,e). All the hydrogen-bonded *R*-Hopa$^-$ helices are left-handed (M). The adjacent 2D $[Ag_2(bpp)_2]_n^{2n+}$ layers are interconnected with a distance of 9.0 Å by the left-handed hydrogen-bonded helices and the third aqua molecules [O1W···O3a = 2.902(6) Å, O1W−H1WB···O3a = 173(7)°; O1W···Ag1 = 2.879 Å, O1W···Ag2 = 3.044 Å] into a chiral sandwich-like supramolecular network in the space group $P2_1$ (Flack parameter: −0.008(6)).

In contrast to 1·3H$_2$O, 1D right-handed (P) homochiral helical chains are found in 2·3H$_2$O [O2W···O2 = 2.765(3) Å, O2W−H2WA···O2 = 159(4)°; O3W···O2W = 2.774(4) Å, O3W−H3WB···O2W = 174(4)°; O3W···O1 = 2.778(4) Å, O3W−H3WA···O1 = 169(5)°] (Figure 1f,g). The right-handedness of the helical obviously originates from the opposite chirality of *S*-Hopa$^-$. The corresponding geometric parameters [Ag1−N = 2.165(3) and 2.171(3) Å, Ag1−O = 2.582(2) Å; Ag1···Ag2 = 2.9835(3) Å] in 2·3H$_2$O are similar to 1·3H$_2$O. Weak interactions between Ag(I) and water oxygen atoms [O1W···Ag1 = 2.880 Å, O1W···Ag2 = 3.040 Å] connect the right-handed hydrogen-bonded helices and achiral $[Ag_2(bpp)_2]_n^{2n+}$ layers to generate a chiral sandwich-like network in a chiral space group $P2_1$ and with absolute structure parameter of −0.06 (1).

Structure of [Ag$_2$(*R*-Hopa)(*S*-Hopa)(bpp)$_2$]·4H$_2$O (3·4H$_2$O). Single crystal X-ray crystallographic analysis reveals that 3·4H$_2$O crystallizes in the space group of $P2_1/c$. The overall network is very similar to chiral 1·3H$_2$O, which is composed of the 2D $[Ag_2(bpp)_2]_n^{2n+}$ layers and Hopa$^-$−H$_2$O helices (Figure 2a). The asymmetric unit contains one silver cation, one bpp in *all-trans*-conformation, one Hopa$^-$ anion, and two guest water molecules. Ag1 is in a heavily distorted tetrahedral coordination geometry surrounded by two bpp ligands and one weakly chelated carboxylate group from Hopa$^-$ [Ag1−N = 2.166(3) and 2.179(3) Å, Ag1−O = 2.644(4) and 2.673(3) Å]. The adjacent $[Ag(bpp)]_n$ chains are linked into a 2D layer by unsupported Ag···Ag interactions in the distance of 3.223(1) Å, longer than those found in 1·3H$_2$O and 2·3H$_2$O (Figure 2b).

Though the crystal structure of racemic 3·4H$_2$O is very similar to chiral 1·3H$_2$O and 2·3H$_2$O in connectivity, successive $[Ag(bpp)]_n^{n+}$ chains within the layer are inversion-related and thus contain alternating enantiomers of the Hopa$^-$. The *R*- and *S*-Hopa$^-$, along with four lattice aqua molecules, form Hopa$^-$−H$_2$O hydrogen bonding chains along the *b*-axis [O3···O1a = 2.894(6) Å, O3−H3···O1a = 154.4°; O2W···O2 = 2.753(7) Å, O2W−H2WA···O2 = 148.8°; O1W···O2 Wb = 2.79 (1) Å, O1W−H1WB···O2 Wb = 159(5)°; O1W···O1 = 2.74(1) Å, O1W−H1WA···O1 = 175(7)°]. Each step of the chain is 8.883(2) Å (Figure 2c). The nonchiral Hopa$^-$−H$_2$O chains, replacing either left-handed in 1·3H$_2$O or right-handed helices in 2·3H$_2$O, are arranged in parallel to link the $[Ag_2(bpp)_2]_n^{2n+}$ layers into a three-dimensional supramolecular network.

Interestingly, the hydroxyl group on the Hopa$^-$ ligand is disordered on two positions at 50%:50% possibility, that is, 50% *R*-Hopa$^-$ and 50% *S*-Hopa$^-$ are found to coordinate to the silver atom in each asymmetric unit. Considering the existence of inversion centers on between two Hopa$^-$ within the hydrogen bonding chains and between the Ag···Ag dimers, two enantiomers form nonchiral Hopa$^-$−H$_2$O chains, which have mirror symmetry to each other, in a statistically 1:1 ratio (Figure 2d).

Structure of [Ag$_2$(*R*-Hopa)(*S*-Hopa)(bpp)$_2$]·H$_2$O (4·H$_2$O). As 4·H$_2$O was yielded from the dehydration of 3·4H$_2$O, it can be expected that both compounds have common structural features. X-ray crystallography revealed that 4·H$_2$O has lower symmetry in space group $P\bar{1}$. The asymmetric unit contains one silver cation, one bpp, one Hopa$^-$, and half a guest water molecule (Figure 3a). Though as found in 3·4H$_2$O, the Ag(I) atom displays a pseudo heavily distorted tetrahedral geometry connected by one Hopa$^-$ and two bpp ligands [Ag1−N = 2.248(2) and 2.239(2) Å], the coordination interactions between the metal centers and carboxylate groups are stronger in 4·H$_2$O [Ag1−O = 2.478(2) and 2.637(2) Å].

1D $[Ag(bpp)]_n^{n+}$ along the *b* axis can still be found in 4·H$_2$O. Nevertheless, the dehydration resulted in the loss of three-quarters of the guest water molecules and smaller void space between the layers. The hydrogen bonding helices formed between two Hopa$^-$ and four water molecules were therefore broken, leading to the moving of $[Ag(bpp)]_n^{n+}$ layers. The dimeric $[Ag_2(bpp)_2]^{2+}$ units linked by weak Ag···Ag interactions in compounds 1−3 were dissociated and the closest

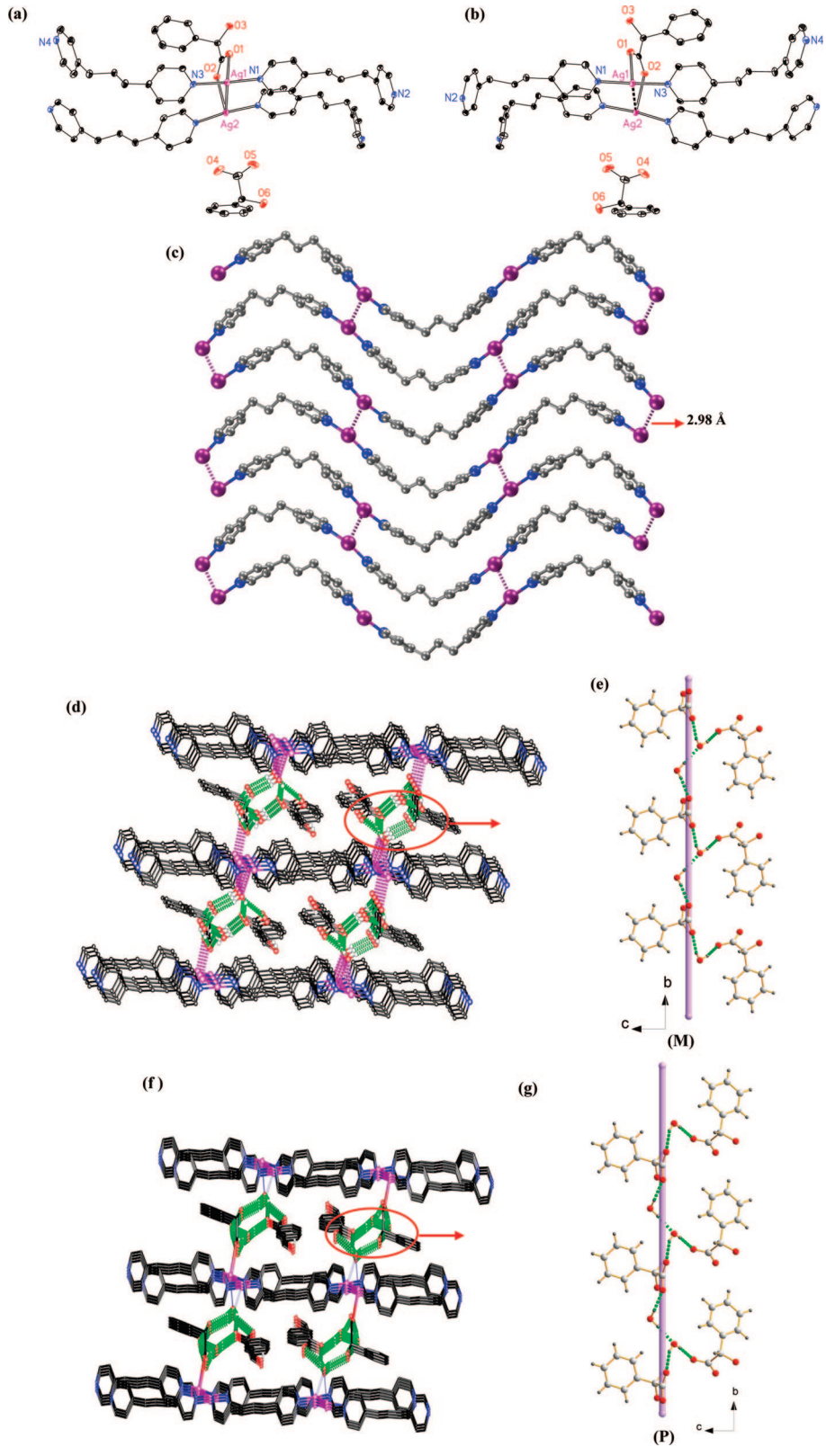

Figure 1. The coordination environment of Ag(I) in **1**·3H_2O (a) and in **2**·3H_2O (b); 2D $[Ag_2(bpp)_2]_n^{2n+}$ structure in **1**·3H_2O or **2**·3H_2O along the *a* axis (c); the sandwich-like network constructed with 2D $[Ag_2(bpp)_2]_n^{2n+}$ layers and the left-handed (*M*) 2_1 helices in **1**·3H_2O along the *b* axis (d); left-handed 2_1 helical hydrogen-bonded chains in **1**·3H_2O along the *a* axis [O2W−H2WA···O2, 2.772(6) Å; O1···H3WB−O3W, 2.776(6) Å; O3W−H3WA···O2W, 2.771(7) Å] (e); the sandwich-like network constructed with 2D $[Ag_2(bpp)_2]_n^{2n+}$ layers and the right-handed (*P*)2_1 helices in **2**·3H_2O along the *b* axis (f); right-handed 2_1 helical hydrogen-bonded chains in **2**·3H_2O along the *a* axis [O2···H2WA−O2W, 2.765(3) Å; O2W···H3WB−O3W, 2.774(4) Å; O3W−H3WA···O1 2.778(4) Å] (g).

Ag···Ag separation between the $[Ag(bpp)]_n^{n+}$ chains extends from 3.223(1) Å in **3**·4H_2O to 4.902 Å in **4**·H_2O (Figure 3b). Analogous to **3**·4H_2O, neighboring $[Ag(bpp)]_n^{n+}$ chains on the silver pyridine layer are centro-symmetric. *R*-Hopa$^-$ and *S*-

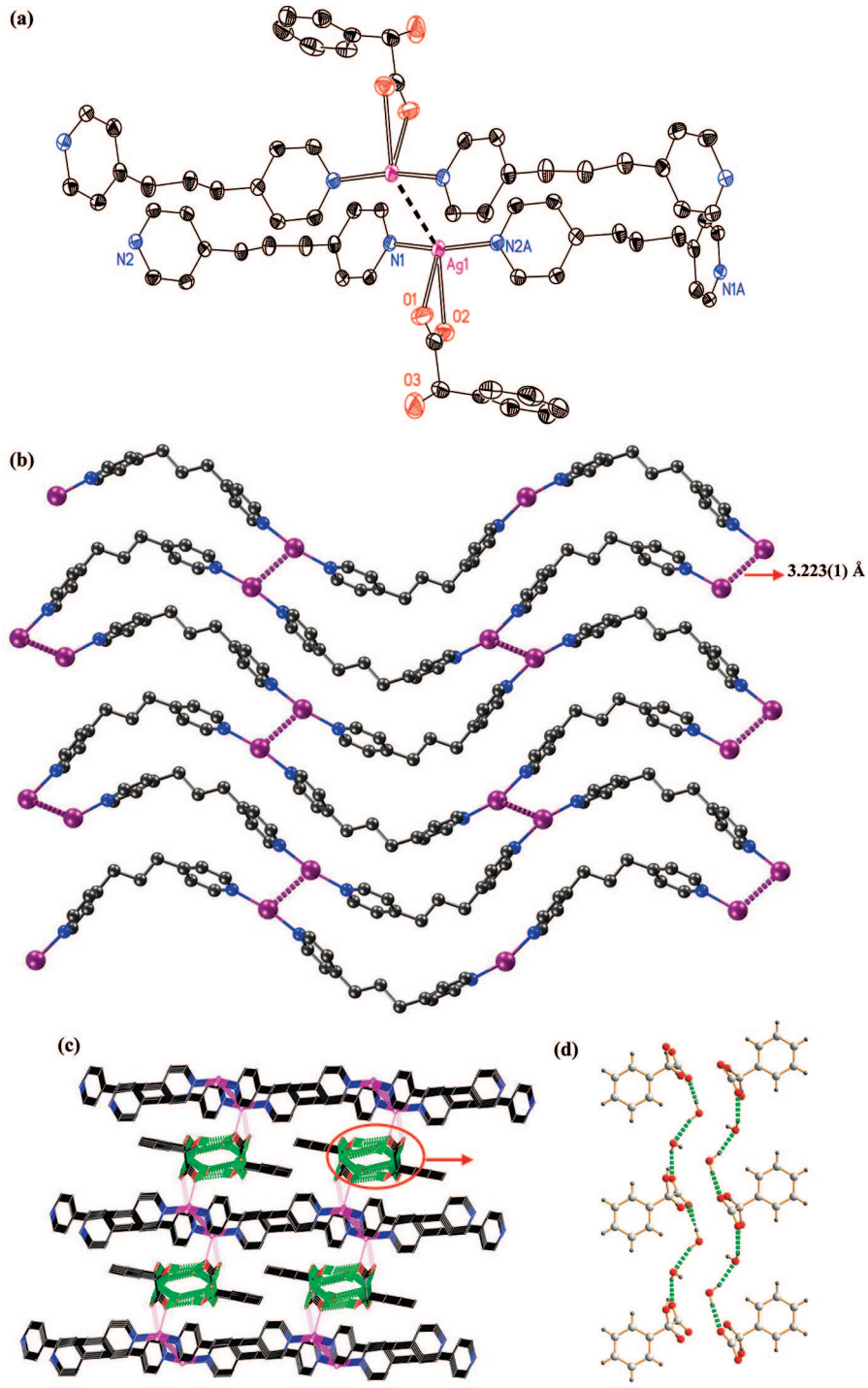

Figure 2. The coordination environment of Ag(I) in **3**·4H_2O (a); 2D $[Ag_2(bpp)_2]_n^{2n+}$ structure in **3**·4H_2O along the *a* axis (b); the sandwich-like network in **3**·4H_2O along the *b* axis (c) and hydrogen-bonded chains in **3**·4H_2O along the *a* axis (d).

$Hopa^-$ stretch alternatively on both sides of the layer and form hydrogen bonds through the hydroxyl and carboxylate groups between the layers [O3···O2 = 2.644(2) Å, O3−H3O···O2 = 118(2)°; O3···O2a = 2.976(2) Å, O3−H3O···O2a = 142(2)°] (Figure 3c). The lattice aqua molecules are situated in between the silver layers and have weak hydrogen interactions with the $Hopa^-$ carboxylate groups, as shown in Figure 3d [O1w···O1 = 2.744(4) Å, O1W−H1WA···O1 = 151.3°; O1W···O1b = 2.919(4) Å, O1W−H1WB···O1b = 151.9°].

Structure of [Ag_2(*R*-Hopa)(*S*-Hopa)(bpp)$_2$]·2MeOH (5·2MeOH). Powder X-ray diffraction showed that **5**·2MeOH is isostructural to **3**·4H_2O, and single crystal X-ray diffraction revealed that **5**·2MeOH has a very similar unit cell in the same space group of $P2_1/c$. Analogous $Ag_2(bpp)_2^{2+}$ dimer and 2D Ag-bpp layers can also be observed in **5**·2MeOH (Figure 4a,b); however, the Ag···Ag distance within the silver dimeric unit contracts from 3.223(1) Å in **3**·4H_2O and 4.902 Å in **4**·H_2O to 2.921(1) Å. The silver atom is also in a heavily distorted tetrahedral coordination geometry and the interaction between Ag and the $Hopa^-$ carboxylate group is pretty weak [Ag1−N = 2.188(1) and 2.200(1) Å, Ag1−O = 2.644(2) and 2.745(1) Å].

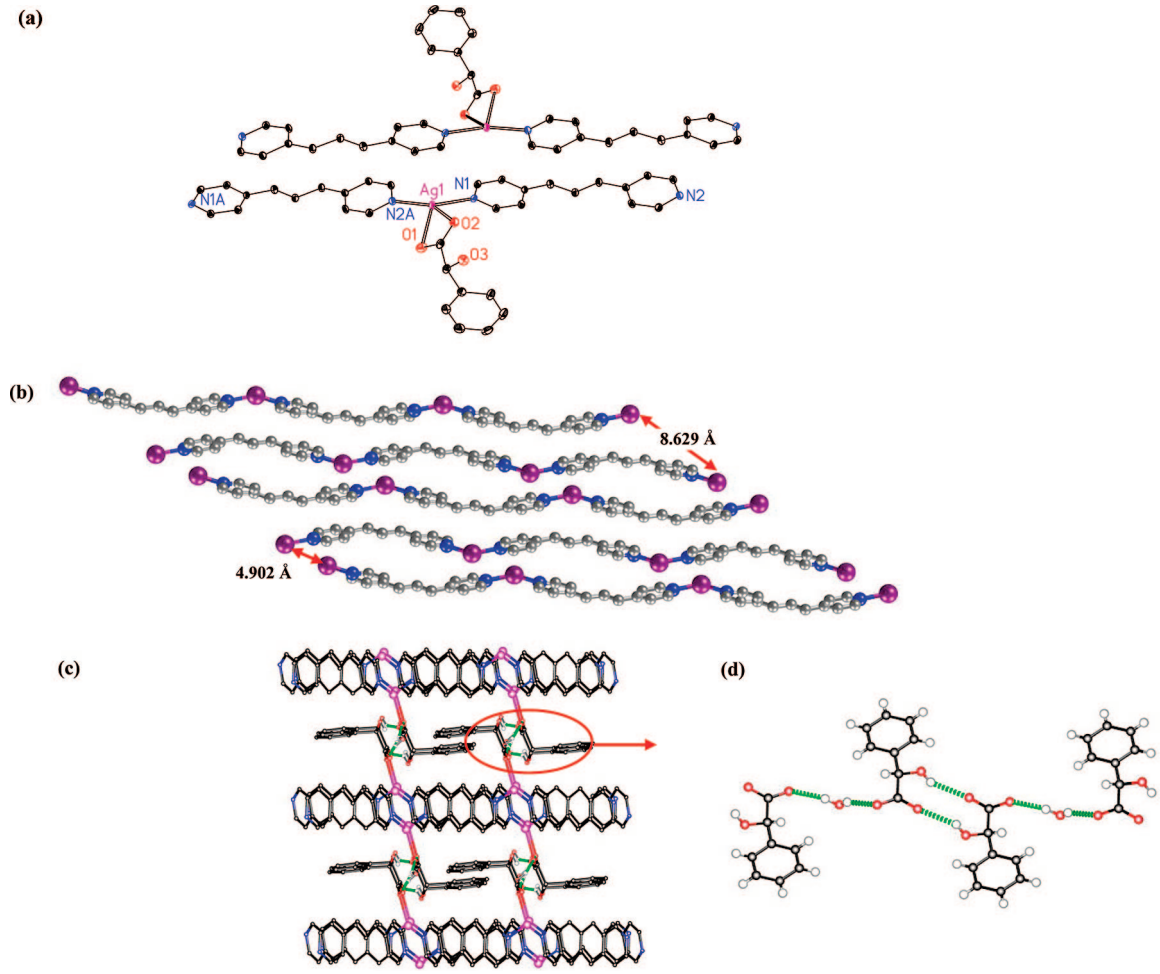

Figure 3. The coordination environment of Ag(I) in **4**·H_2O (a); parallel linear $[Ag(bpp)]_n^{n+}$ structure in **4**·H_2O along the *a* axis (b); the sandwich-like network in **4**·H_2O along the *b* axis (c); and the centrosymmetric hydrogen-bonded guest *R*-$Hopa^-$−H_2O−*S*-$Hopa^-$ arrangement in **4**·H_2O (d).

Adjacent $[Ag_2(bpp)_2]_n^{2n+}$ layers are interconnected by *rac*-$Hopa^-$ and MeOH into sandwich-like supramolecular network (Figure 4c). The hydrogen-bonded chain is composed of alternative *R*-$Hopa^-$···MeOH and *S*-$Hopa^-$···MeOH [O4···O2 = 2.739(5) Å, O4−H4o···O2 = 155°] (Figure 4d). The suitable size of the volume between the layers and the existence of hydroxyl group on $Hopa^-$ may account for the affinity of the framework for methanol.

Phase Transformation Discussion. Phase transformation based on flexible networks is one of the most interesting phenomena in coordination polymers though the understanding of their mechanisms is still a big challenge. The versatile hydrogen bonds between $Hopa^-$ and the lattice water or MeOH molecules are essential for the dynamic structural transformations among **3**·$4H_2O$, **4**·H_2O, and **5**·2MeOH via partial dehydration, readsorption, and guest-exchange. The suitable size and the affinity for hydrogen bonds may account for the selective absorption of methanol in the mixed MeOH−EtOH−DMF solvent for **4**·H_2O. The exchange of the lattice methanol in **5**·2MeOH to water in **4**·H_2O in wet air may be due to the easy volatility of methanol and greater affinity of aqua for hydrogen bonds. The dehydration and exchange of the guest molecules give rise to the breakage and reformation of hydrogen bonding chains, which leads to the reversible slipping movement of $[Ag(bpp)]_n^{n+}$ chains on the $[Ag_2(bpp)_2]_n^{2n+}$ layers in these compounds.

TGA Characterization. Thermogravimetric analysis shows that **1**−**5** have similar thermal stability. The first weight loss at below 100 °C was observed for all the compounds, which is in accordance with the loss of lattice water or methanol molecules. The networks began to decompose at above 150 °C (Figure 5). For **1**·$3H_2O$ and **2**·$3H_2O$, the observed weight loss (5.35%) at 60 °C is corresponding to the removal of three guest water molecules (5.58%); for **3**·$4H_2O$, the release of four water molecules per formula was observed under 80 °C (observed 7.20%, calcd: 7.31%); for **4**·H_2O, the removal of one lattice water molecule (1.84%) occurred at 105 °C with the observed weight loss of 1.91%; for **5**·2MeOH, two guest methanol molecules escaped from the network under 85 °C (observed 6.29%, calcd. 6.87%).

Solid-state CD spectra. The solid-state CD Spectra of **1**·$3H_2O$ and **2**·$3H_2O$ are given in Figure 6.

The bulky crystalline sample of **1**·$3H_2O$ in a KCl pellet displays negative Cotton effects at the band of about 205−230 nm. And the CD signal of **2**·$3H_2O$ sample is the mirror image of **1**·$3H_2O$. The results of CD measurements show the enantiopurity of **1**·$3H_2O$ and **2**·$3H_2O$, confirming that H_2opa keep their chirality under these reaction conditions.[30,31]

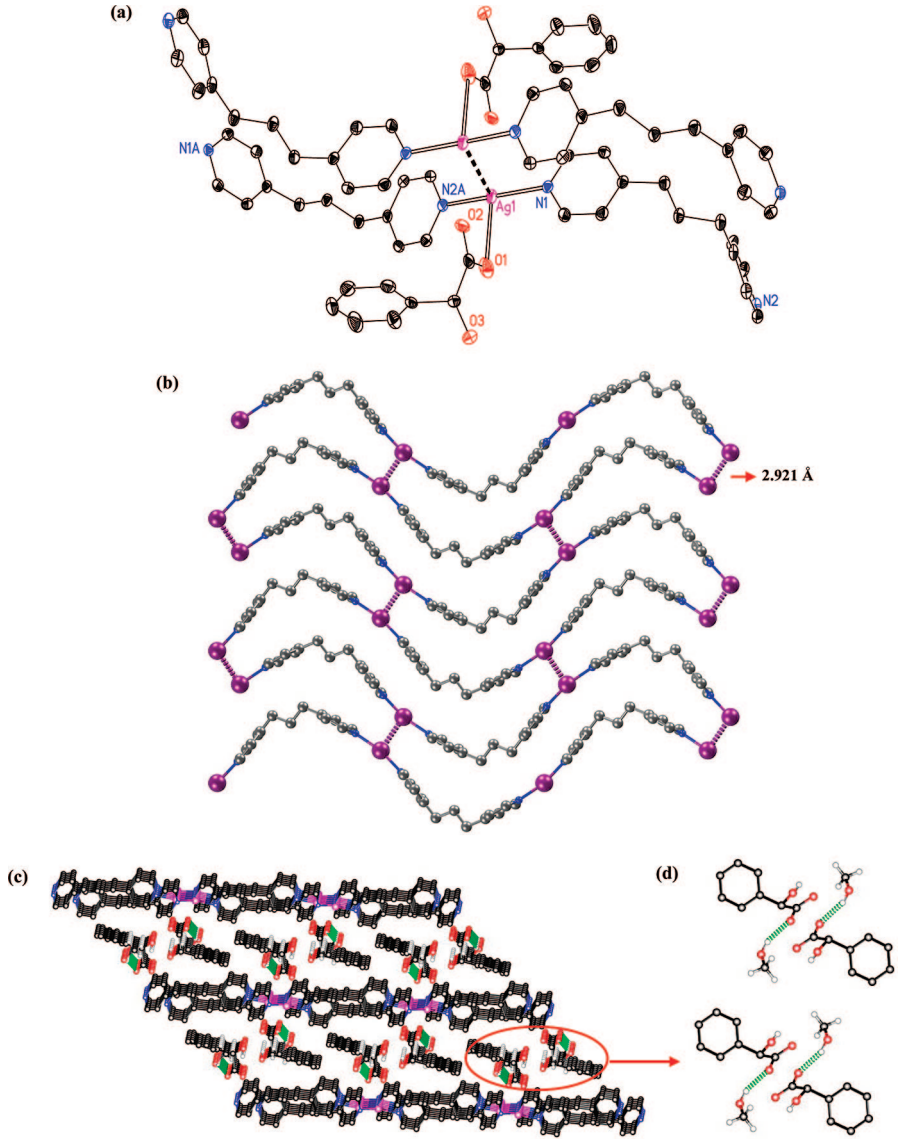

Figure 4. The coordination environment of Ag(I) in **5**·2MeOH (a); 2D $[Ag_2(bpp)_2]_n^{2n+}$ structure in **5**·2MeOH along the *a* axis (b); the sandwich-like network in **5**·2MeOH along the *b* axis (c) and the centrosymmetric hydrogen-bonded MeOH−Hopa$^-$ (O4−H4B···O2, 2.738(1) Å) arrangement in **5**·2MeOH (d).

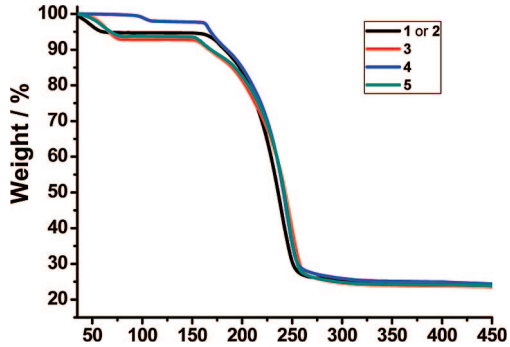

Figure 5. TG curves for **1**−**5**.

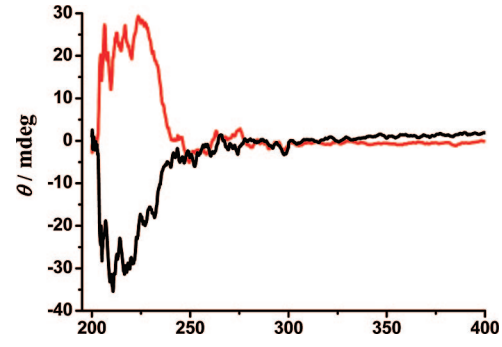

Figure 6. The solid-state CD Spectra of **1**·3H_2O (black line) and **2**·3H_2O (red line).

Conclusion

Two enantiopure and one racemic Ag-bpp-Hopa$^-$ sandwich-like supramolecular networks, **1**·3H_2O, **2**·3H_2O, and **3**·4H_2O, have been prepared and characterized. All the compounds have analogous $[Ag_2(bpp)_2]_n^{2n+}$ coordination layers connected by Hopa$^-$−H_2O hydrogen bonding chains. In **1**·3H_2O and **2**·3H_2O, *R*-Hopa$^-$ or *S*-Hopa$^-$ form left-handed or right-handed helices with water molecules running in parallel to the Ag-bpp layers while in **3**·4H_2O, the centrosymmetric hydrogen bonding chains are composed of two enantiomers of Hopa$^-$.

Upon dehydration, readsorption and selective guest-exchange, reversible phase transformation of **3**·4H_2O was observed. The Ag···Ag dimeric units in $[Ag_2(bpp)_2]_n^{2n+}$ in **3**·4H_2O were broken and new Hopa$^-$−H_2O chains between the silver layers

were formed in **4**·H_2O by adjusting the positions of the Ag-bpp chains when there is less lattice aqua molecules. After absorbing methanol, the Ag-bpp chains restored to their original layer structures in **5**·2MeOH. The different structural features can be ascribed to different hydrogen bonding interactions between $Hopa^-$ and the lattice water or MeOH molecules.

Acknowledgment. This work was supported by the NSFC (Grant nos. 20525102, 20821001, and J0730420), the "973 Project" (2007CB815305), and the Scientific and Technological Project of Guangdong Province (04205405). Zhuojia Lin thanks Sun Yat-Sen University for 'One hundred Talent' funding.

Supporting Information Available: X-ray crystallographic files (CIF), hydrogen bonds distances and angles of **1**−**5** and solid-state CD Spectra of *R*-H_2opa and *S*-H_2opa. This material is available free of charge via the Internet at http://pubs.acs.org.

References

(1) Seo, J. S.; Whang, D.; Lee, H.; Jun, S. I.; Oh, J.; Jeon, Y. J.; Kim, K. *Nature* **2000**, *404*, 982.
(2) Vaidhyanathan, R.; Bradshaw, D.; Rebilly, J. N.; Barrio, J. P.; Gould, J. A.; Berry, N. G.; Rosseinsky, M. J. *Angew. Chem., Int. Ed.* **2006**, *45*, 6495.
(3) (a) Burrows, A.; Harrington, R. W.; Mahon, M. F.; Teat, S. J. *Eur. J. Inorg. Chem.* **2003**, 766. (b) ThuLry, P. *Eur. J. Inorg. Chem.* **2006**, 3646. (c) Zeng, M.-H.; Wang, B.; Wang, X.-Y.; Zhang, W.-X.; Chen, X.-M.; Gao, S. *Inorg. Chem.* **2006**, *45*, 7069.
(4) (a) Wu, C.-D.; Hu, A.; Zhang, L.; Lin, W.-B. *J. Am. Chem. Soc.* **2005**, *127*, 8940. (b) Kesanli, B.; Cui, Y.; Smith, M. R.; Bittner, E. W.; Bockrath, B. C.; Lin, W.-B. *Angew. Chem., Int. Ed.* **2005**, *44*, 72. (c) Li, G.; Yu, W.; Ni, J.; Liu, T.; Liu, Y.; Sheng, E.; Cui, Y. *Angew. Chem., Int. Ed.* **2008**, *47*, 1245. (d) Liu, Y.; Xu, X.; Zheng, F.; Cui, Y. *Angew. Chem., Int. Ed.* **2008**, *47*, 4538.
(5) Lluïsa, P.-G.; David, B. A. *Chem. Soc. Rev.* **2002**, *31*, 342.
(6) (a) Xiong, R.-G.; You, X.-Z.; Abrahams, B. F.; Xue, Z.; Che, C.-M. *Angew. Chem., Int. Ed.* **2001**, *40*, 4422. (b) Guillou, N.; Livage, C.; Drillon, M.; Ferey, G. *Angew. Chem., Int. Ed.* **2003**, *42*, 5314.
(7) (a) Serre, C.; Millange, F.; Surble, S.; Greneche, J.-M.; Ferey, G. *Chem. Mater.* **2004**, *16*, 2706. (b) Lin, Z.; Slawin, A. M. Z.; Morris, R. E. *J. Am. Chem. Soc.* **2007**, *129*, 4880.
(8) Ezuhara, T.; Endo, K.; Aoyama, Y. *J. Am. Chem. Soc.* **1999**, *121*, 3279.
(9) Wu, S.-T.; Wu, Y.-R.; Kang, Q.-Q.; Zhang, H.; Long, L.-S.; Zheng, Z.-P.; Huang, R.-B.; Zheng, L.-S. *Angew. Chem., Int. Ed.* **2007**, *46*, 8475.
(10) Tian, G.; Zhu, G.-S.; Yang, X.-Y.; Fang, Q.-R.; Xue, M.; Sun, J.-Y.; Wei, Y.; Qiu, S.-L. *Chem. Commun.* **2005**, 1396.
(11) Li, M.-X.; Sun, Q.-Z.; Bai, Y.; Duan, C.-Y.; Zhang, B.-G.; Meng, Q.-J. *Dalton Trans.* **2006**, 2572.
(12) Khatua, S.; Stoeckli-Evans, H.; Harada, T.; Kuroda, R.; Bhattacharjee, M. *Inorg. Chem.* **2006**, *45*, 9619.
(13) Ademi, L.; Constable, E. C.; Housecroft, C. E.; Neuburger, M.; Schaffner, S. *Dalton Trans.* **2003**, 4565.
(14) Islas, J. R.; Lavabre, D.; Grevy, J.; Lamoneda, R. H.; Cabrera, H. R.; Micheau, J.; Buhse, T. *Proc. Natl. Acad. Sci. U. S. A.* **2005**, *102*, 13743.
(15) (a) For examples: Dybtsev, D. N.; Chun, H.; Kim, K. *Angew. Chem., Int. Ed.* **2004**, *43*, 5033. (b) Biradha, K.; Fujita, M. *Angew. Chem., Int. Ed.* **2002**, *41*, 3392. (c) Abrahams, B. F.; Hardie, M. J.; Hoskins, B. F.; Robson, R.; Williams, G. A. *J. Am. Chem. Soc.* **1992**, *114*, 10641. (d) Kitagawa, S.; Uemura, K. *Chem. Soc. Rev.* **2005**, *34*, 109. (e) Vittal, J. J. *Coord. Chem. Rev.* **2007**, *251*, 1781. (f) Halder, G. J.; Kepert, C. J. *Aust. J. Chem.* **2006**, *59*, 597. (g) Kawano, M.; Fujita, M. *Coord. Chem. Rev.* **2007**, *251*, 2592. (h) Kepert, C. J.; Rosseinsky, M. J. *Chem. Commun.* **1999**, 375. (i) Li, H.-L.; Eddaoudi, M.; O'Keeffe, M.; Yaghi, O. M. *Nature* **1999**, *402*, 276. (j) Maji, T. K.; Uemura, K.; Chang, H.-C.; Matsuda, R.; Kitagawa, S. *Angew. Chem., Int. Ed.* **2004**, *43*, 3269. (k) Cheng, X.-N.; Zhang, W.-X.; Lin, Y.-Y.; Zheng, Y.-Z.; Chen, X.-M. *Adv. Mater.* **2007**, *19*, 1494. (l) Kaneko, W.; Ohba, M.; Kitagawa, S. *J. Am. Chem. Soc.* **2007**, *129*, 13706. (m) Xue, D.-X.; Zhang, W.-X.; Chen, X.-M.; Wang, H.-Z. *Chem. Commun.* **2008**, 1551.
(16) Suh, M. P.; Ko, J. W.; Choi, H. J. *J. Am. Chem. Soc.* **2002**, *124*, 10976.
(17) Wu, C.-D.; Lin, W.-B. *Angew. Chem., Int. Ed.* **2005**, *44*, 1958.
(18) Zeng, M.-H.; Feng, X.-L.; Chen, X.-M. *Dalton Trans.* **2004**, 2217.
(19) Bradshaw, D.; Warren, J. E.; Rosseinsky, M. J. *Science* **2007**, *315*, 977.
(20) Takaoka, K.; Kawano, M.; Tominaga, M.; Fujita, M. *Angew. Chem., Int. Ed.* **2005**, *44*, 2151.
(21) Hu, C.-H.; Englert, U. *Angew. Chem., Int. Ed.* **2005**, *44*, 2281.
(22) (a) Niel, V.; Thompson, A. L.; Muñoz, M. C.; Galet, A.; Goeta, A. E.; Real, J. A. *Angew. Chem., Int. Ed.* **2003**, *42*, 3760. (b) Zhang, J.-P.; Lin, Y.-Y.; Zhang, W.-X.; Chen, X.-M. *J. Am. Chem. Soc.* **2005**, *127*, 14162.
(23) (a) Tong, M.-L.; Chen, X.-M.; Ng, S. W. *Inorg. Chem. Commun.* **2000**, *3*, 436. (b) Tong, M.-L.; Wu, Y.-M.; Ru, J.; Chen, X.-M.; Chang, H.-C.; Kitagawa, S. *Inorg. Chem.* **2002**, *41*, 4846.
(24) Sheldrick, G. M. *SADABS 2.05*, University of Göttingen.
(25) SHELXTL 6.10, Bruker Analytical Instrumentation, Madison, Wisconsin, USA, 2000.
(26) (a) Zhao, X. L.; Wang, Q. M.; Mak, T. C. W. *Chem. Eur. J.* **2005**, *11*, 2094. (b) Zhang, X.; Guo, G. C.; Zheng, F. K.; Zhou, G. W.; Mao, J. G.; Dong, Z. C.; Huang, J. S.; Mak, T. C. W. *J. Chem. Soc., Dalton Trans.* **2002**, 1344. (c) Wu, D. D.; Mak, T. C. W. *J. Chem. Soc., Dalton Trans.* **1995**, 2671. (d) Chen, X. M.; Mak, T. C. W. *J. Chem. Soc., Dalton Trans.* **1991**, 3253. (e) Chen, X. M.; Mak, T. C. W. *J. Chem. Soc., Dalton Trans.* **1991**, 1219.
(27) Smith, G.; Reddy, A. N.; Byriel, K. A.; Kennard, C. H. L. *J. Chem. Soc., Dalton Trans.* **1995**, 3565.
(28) Michaelides, A.; Kiritsis, V.; Skoulika, S.; Aubry, A. *Angew. Chem., Int. Ed. Engl.* **1993**, *32*, 1495.
(29) (a) Wang, J.; Hu, S.; Tong, M.-L. *Eur. J. Inorg. Chem.* **2006**, 2069. (b) Tan, C.-K.; Wang, J.; Leng, J.-D.; Zheng, L.-L.; Tong, M.-L. *Eur. J. Inorg. Chem.* **2008**, 771.
(30) Zeng, M.-H.; Gao, S.; Chen, X.-M. *Inorg. Chem. Commun.* **2004**, *7*, 864.
(31) Beghidja, A.; Hallynck, S.; Welter, R.; Rabu, P. *Eur. J. Inorg. Chem.* **2005**, 662.
(32) Bondi, A. J. *J. Phys. Chem.* **1964**, *68*, 441.
(33) Pyykkö, P. *Chem. Rev.* **1997**, *97*, 597.

CG800710Q